Heterogeneous Timing of Gene Induction as a Regulation Strategy

Georg Fritz [1,*], **Noreen Walker** [2] **and Ulrich Gerland** [3,*]

*1 - **LOEWE Center for Synthetic Microbiology & Department of Physics,** Marburg, Germany*
*2 - **Max Planck Institute of Molecular Cell Biology and Genetics,** Dresden, Germany*
*3 - **Physik Department,** Technische Universität München, Garching, Germany*

***Correspondence to Georg Fritz and Ulrich Gerland:**. georg.fritz@synmikro.uni-marburg.de, gerland@tum.de*
https://doi.org/10.1016/j.jmb.2019.05.020
Edited by Kirsten Jung

Abstract

In response to environmental changes, cells often adapt by up-regulating genes to synthesize proteins that generate a benefit in the new environment. Several such cases of gene induction have been reported where the timing was heterogeneous, with some cells responding early and others responding late, although the microbial population was genetically homogeneous and the environment was well mixed. Here, we explore under which conditions heterogeneous timing of gene induction could be advantageous for the population as a whole. We base our study on a mathematical model that accounts for the cost of protein synthesis in terms of resources, which cells must provide immediately, whereas the associated benefit accumulates only slowly over the protein lifetime. Due to this delayed benefit, gene induction can be a risky investment, if resources are scarce and the environment fluctuates rapidly and unpredictably. Unprofitable gene induction then depletes the remaining limiting resource needed for maintenance of cell viability. We show that whenever gene induction is associated with a transient risk but beneficial in the long run, the stochastic timing of gene induction maximizes the reproductive success of a population. In particular, in an environment of stochastic periods of famine and feast, an optimum emerges from a trade-off between short-term growth, favoring rapid and homogeneous responses, and long-term survival, favoring a broadly heterogeneous response. Our analysis suggests that the optimal variability of induction times is just as large as the time required for the amortization of the initial investment into protein synthesis.

Introduction

It has long been known that colonies of genetically identical microbes in homogeneous environments can display substantial cell-to-cell variability in gene expression states [1,2]. Such phenotypic heterogeneity has been characterized with modern single-cell methods in a range of microbial systems [3–5]. While noise is omnipresent in gene regulatory circuits [6], such that phenotypic heterogeneity is easy to produce, the intriguing question arises whether noise is only a necessary evil or also plays a functional role [7–11]. One expects phenotypic heterogeneity to be useful as a diversification strategy in risky environments ("bet-hedging") [5,12–15] or as a division-of-labor strategy in bacterial communities [16–18]. An example for microbial bet-hedging is bacterial persistence, where a clonal population of *Escherichia coli* copes with unpredictable exposures to antibiotics by stochastically switching between a slow-growing resistant and a fast-growing non-resistant phenotype [12]. More generally, a strategy of stochastic switching between phenotypes is beneficial for genetic systems that alleviate sudden severe stresses [19,20].

However, most gene regulatory systems in microbes appear to implement a responsive switching strategy. Typically, a signaling system senses an environmental cue and elicits a gene-regulatory response, for example, up-regulation of a set of genes. A paradigmatic example of responsive switching is the induction of carbon utilization systems for sugars such as lactose, arabinose, or galactose [1,4,21–23]. There are several

reports of a specific type of phenotypic heterogeneity that occurs during responsive switching: cells that responsively switch do so at different points in time, although they are genetically identical and in the same well-mixed environment (see Fig. 1). We refer to this type of phenotypic heterogeneity as "heterogeneous timing." Examples of heterogeneous timing include the induction of the arabinose uptake system in *E. coli* [3,24,25], the kinetics of genetic switching into the state of bacterial competence [26], and the timing of sporulation after starvation in *Bacillus subtilis* [27]. Heterogeneous timing is also observed in growth resumption after stationary phase (see Ref. [28] and references therein). The time delay between early and late responders varies from case to case, but can be several tens of minutes or even hours. The phenomenon of heterogeneous timing is clear-cut only if the spread in the switching time points is larger than the time required for the switching process in a single cell. For instance, in the case of the arabinose uptake system, this is true only at low concentrations of external arabinose [24,25].

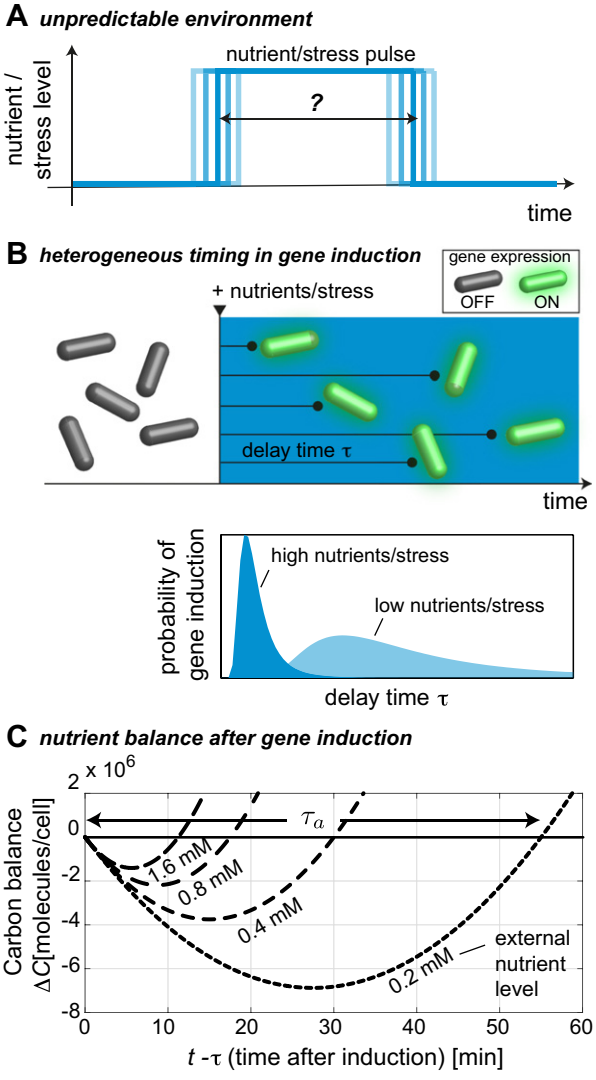

Fig. 1. Heterogeneous timing and amortization of gene induction. (A) Environment that offers limited amounts of resources in unpredictable pulses. (B) Observed single-cell behavior: different cells induce genes to adapt to new environment at different points in time. (C) Intracellular carbon balance after gene induction, as described by Eq. (2), reveals a finite amortization time τ_a for varying substrate concentrations. The amortization time τ_a is marked for 0.2 mM external sugar.The parameter values are adapted to the arabinose utilization system of *E. coli* [24], including a cost factor of α = 5000 resource molecules per functional unit and a benefit from arabinose uptake at rate $v_S = v_{max}S/(K_m + S)$, with v_{max} = 2000 resource molecules/min, K_m = 2 mM and k_p = 100 copies/min.

It is currently unknown whether heterogeneous timing is a regulation strategy, that is, whether it confers a selective advantage to microbes. The purpose of this paper is to point out that heterogeneous timing *can* be advantageous under certain conditions, which we want to clarify. The costs associated with gene induction [29–33] play an important role in our analysis. Our approach is based on a coarse-grained mathematical model for microbial growth in unpredictable fluctuating environments, which takes these costs into account. Intuitively, the advantage of heterogeneous timing arises as follows within this model.

First, consider environmental conditions in which the cost of protein synthesis in terms of resources is significant. For instance, after all carbon sources have been depleted, both energy and amino acids will be scarce. Under such conditions, any protein synthesis constitutes a resource investment for the cell. Now, consider a change in the environmental conditions to a state, in which the induction of a set of genes is beneficial for the cell. For instance, a new carbon source becomes suddenly available, for the usage of which the associated carbon utilization system needs to be expressed. Or, a new stress arises, under which the induction of a stress response system reduces the rate of cell death. Importantly, the cell can sense the change in the environment, but it cannot know, a priori, how long the new carbon source or the stress factor will be around (Fig. 1A). Furthermore, protein synthesis will incur an immediate cost in terms of the limiting resources, while the associated enzymatic benefit will be obtained after a delay, and only gradually over the lifetime of the proteins. What matters for the cell is the net resource balance, that is, the total benefit obtained from the enzymatic activity minus the resource cost for protein synthesis. After gene induction, this net resource balance will be time dependent. In particular, the balance will transiently be negative due to the delayed and gradual benefit. In case the environment remains in the new state for a sufficiently long period, the net balance will ultimately become positive for the cell, such that

the investment in protein synthesis pays off. If, however, the environment changes again before the balance becomes positive, gene induction was unprofitable for the cell and effectively depletes its remaining resources needed for maintenance of viability. In this case, heterogeneous timing of gene induction works as a bet-hedging strategy that maximizes the reproductive success of a population of cells, as the analysis of our model will show.

This paper is organized as follows. We first take the qualitative cost–benefit consideration above to a quantitative level. This will lead us to the definition of an amortization time for the production of enzymes, a central concept for our interpretation of heterogeneous timing as a regulation strategy. Based on the amortization time concept, we then formulate two different coarse-grained models for microbial growth and survival in fluctuating environments. First, we consider a model that is minimal, in the sense that it reduces the broad spectrum of delay times of cells into only two classes of behavior, "quick response" *versus* "slow response," and it considers only two classes of environmental fluctuations, 'short pulse' *versus* "long pulse." This minimal description makes the bet-hedging mechanism implemented by heterogeneous timing transparent, by capturing the trade-off between short-term growth, favoring rapid and homogeneous responses, and long-term survival. As the model of Kussell and Leibler [20] for the case of stochastic switching, our minimal model is analytically solvable and serves the purpose of elucidating the essence of the phenomenon. Our second model then stays closer to the observed phenomenology, by allowing for a continuous range of delay times, as well as a continuous range of environmental fluctuations. The analysis of this model explicitly demonstrates that the optimal variability of induction times is just as large as the amortization time. Finally, we discuss a mechanism producing heterogeneous timing in gene induction, which is inferred from the regulatory design and behavior of the arabinose uptake system of *E. coli*. The underlying regulatory scheme is simple and could be implemented in different ways in synthetic and other natural systems.

Results

Amortization time for the production of enzymes

According to the intuitive argument given in the introduction, the adaptation to a changed environment by inducing a set of genes can lead to a transient period of negative resource balance associated with this set of genes. We will now put this argument on a more systematic basis to address four pertinent questions: (i) Under which conditions, if any, will such a transient negative resource balance indeed emerge? (ii) If it does emerge, how long can we expect this transient period to be? (iii) How severe could this effect be; that is, what is the maximal resource loss? (iv) What are the key parameters that determine these two characteristics, that is, the duration and the maximal loss?

For our analysis, we consider a scenario where prior to the environmental change, cells are in a non-growing state, in which they only have access to a limited pool of building blocks and energy carriers. We will characterize the average size of this pool by a single time-dependent quantity, $C(t)$, measuring the number of available resource molecules per cell (see below). We assume that the environment changes to a state, in which the expression of a previously repressed set of genes produces a benefit. To be concrete, we will consider the case where a new carbon source becomes suddenly available, and the set of genes encodes the corresponding carbon utilization system. Note that our model and analysis are by no means limited to this case, as discussed further below. The point in time when the environmental change occurs is random and unpredictable for cells, as is the duration for which the new carbon source remains available (Fig. 1A). We are interested in the dynamic resource balance associated with the new carbon utilization system, that is, the time-dependent difference $\Delta C(t)$ between the benefits and the costs produced by this system. It will be convenient to measure $\Delta C(t)$ in terms of the number of carbon carrying nutrient molecules, which this system imports and catabolizes. For the calculation of $\Delta C(t)$, we choose the time of the environmental change as the reference point, $t = 0$, and denote the time delay after which the set of genes is induced by $\tau \geq 0$. Hence, heterogeneous timing within our model means that different cells display different τ values, resulting in a distribution $P(\tau)$ over the population of cells (Fig. 1B).

To obtain $\Delta C(t)$, we separately consider the costs and benefits produced by the induction of the carbon utilization system, similar to previous studies [30,31]. After induction at time $t = \tau$, the associated proteins are synthesized at rate k_p. A cell then has on average $(t - \tau)\, k_p$ uptake proteins at time t, each of which imports carbon substrate molecules at an uptake rate v_S, thereby increasing $\Delta C(t)$ at rate $(t - \tau)\, k_p \cdot v_S$. In parallel, nutrient molecules are consumed for protein synthesis. Denoting by α the number of nutrient molecules required to synthesize one functional unit of the carbon utilization system, we obtain

$$\frac{d}{dt}\Delta C(t) = (t-\tau)\, k_p \cdot v_S - k_p\, \alpha \qquad (1)$$

for $t > \tau$. In this dynamic equation for the resource balance $\Delta C(t)$, the first term on the right hand side

corresponds to the benefit generated by the enzymes of the carbon utilization system, while the second term represents the metabolic cost of protein expression. In principle, further costs arise from gene expression, in particular for mRNA synthesis [33]. However, since these costs are also proportional to the gene expression rate, we will simply absorb them into the effective cost parameter α. In addition, enzymes can have significant costs incurred by their activity [32]. We will assume that any such costs are accounted for by a reduction of the benefit, which is also coupled to the activity of the enzymes. Hence, v_S will be an effective parameter quantifying the net benefit from enzymatic activity. From Eq. (1), we obtain a parabolic from for the dynamics of the resource balance $\Delta C(t)$ after gene induction ($t > \tau$),

$$\Delta C(t) = \frac{k_p v_S}{2}(t-\tau)^2 - k_p\,\alpha\cdot(t-\tau). \qquad (2)$$

Figure 1C shows exemplary $\Delta C(t)$ curves, with parameter values that we will discuss further below. Equation (2) predicts that there is always a transient period during which cells invest more resources for gene induction than they gain from the expressed proteins, that is, $\Delta C(t) < 0$. We refer to the duration of this period,

$$\tau_a = \frac{2\,\alpha}{v_S}, \qquad (3)$$

as the amortization time for the production of enzymes, since after this time, the enzymes have catabolized as many resource molecules as are required to build them.

The notion of an amortization time for the production of enzymes is more general than suggested by our example of the carbon utilization system. In other cases where the expression of a functional set of genes produces a benefit, quantified by the effective benefit parameter v_S, while incurring a cost measured by α, the amortization time takes on the same form as Eq. (3), provided that v_S and α are expressed in appropriate units (otherwise an additional conversion factor appears). On an intuitive level, the form of Eq. (3) arises simply by dividing the cost by the effective speed of recovering it, where the factor two stems from the fact that the enzymes have been gradually produced over the entire period and have, on average, only worked for half that period.

In going forward with our analysis, it will be important to have an estimate of the absolute timescales that we can expect for the amortization time τ_a. For this estimate, we again use the example of a carbon utilization system. What is the metabolic cost α for the synthesis of such a system? It was previously estimated that for each amino acid in a protein, *E. coli* consumes on average 1.2 to 4.5 carbon carrying resource molecules (for growth on glucose and acetate, respectively) [34]. This estimate includes all the different metabolic costs, for material as well as energy. Using this estimate, the total cost for synthesizing a protein of the average size of 360 amino acids [35] is 430 to 1620 resource molecules. We will therefore use 1000 molecules per protein as a typical value. Carbon utilization systems typically comprise a number of specific proteins for the uptake of the carbon source and its initial degradation before central metabolic pathways can process the resulting products. For instance, L-arabinose utilization in *E. coli* involves seven specific proteins, the arabinose-proton symporter AraE, an ABC transporter consisting of AraF, AraG and AraH, the arabinose–isomerase AraA, the ribulokinase AraB, and the ribulose-5-phosphate-epimerase AraD. The end product of this functional unit is D-xylulose 5-phosphate, which can be processed in the pentose phosphate pathway. To obtain a conservative estimate for the total cost α, we assume five proteins of typical size per functional unit, which yields $\alpha \sim 5000$ resource molecules.

Next, we seek the typical range of v_S, the rate at which a functional unit of the carbon utilization system takes up and processes resource molecules. We focus on the uptake, since flux balance requires that the downstream processing flux matches the uptake flux. The latter depends on the external carbon substrate concentration S via a Michaelis–Menten relation,

$$v_S = v_{\max}\frac{S}{K_m + S}, \qquad (4)$$

with the maximal uptake rate $v_{\max}$ and the Michaelis constant K_m. Using the arabinose and lactose systems as exemplary cases, the maximal uptake rates per transporter are in the range $v_{\max} = 1000$ to 3000 molecules per minute [36–38]. At saturating substrate levels, $S \gg K_m$, Eq. (3) then predicts amortization times in the range of 3 to 10 min. However, carbon utilization systems are typically induced at much lower external concentrations S. For instance, the arabinose and lactose systems are induced already when their transporters operate at ~10% of their $v_{\max}$ values. At these sub-saturating substrate levels, Eq. (3) predicts substantial amortization times τ_a in the range of 30 to 100 min. The resource balance curves $\Delta C(t)$ shown in Fig. 1C plot Eq. (2) with parameters adapted for the arabinose utilization system (see caption), for different concentrations S of external arabinose. These curves illustrate how the amortization time scale grows with decreasing external arabinose concentration (and thus decreasing uptake rate).

Maximal resource loss due to unprofitable gene induction

The other important characteristic of the resource balance curves $\Delta C(t)$ is the minimum that is reached

after half of the amortization time has passed (see Fig. 1C). This minimum represents the maximal loss of resources for a cell, in case the environment changes again, to a state where the newly induced set of genes is no longer beneficial. From Eq. (2), we obtain an expression for the minimum of $\Delta C(t)$ in terms of our model parameters,

$$\Delta C_{\min} = -\frac{k_p\, a^2}{2\, v_S}. \qquad (5)$$

Clearly, for the economics of a cell, it is relevant how this maximal deficit relates to the total amount of resources that remain available to the cell. If $\Delta C_{\min}$ is only a tiny fraction of the resource reserves, then a cell can tolerate many unprofitable gene inductions, whereas the maximal deficit constitutes a considerable risk, if it is a large fraction of those reserves.

The maximal deficit, $\Delta C_{\min}$, depends on the external substrate concentration via v_S according to Eq. (4). Typically, cells also adjust the induction level k_p as a function of the substrate concentration S. In the case of the arabinose utilization system (Fig. 1C), the maximal induction level is reached already at S much below the K_m of the uptake system [25], such that the maximal deficit increases with decreasing substrate concentration. For instance, at 0.4 mM of external sugar, Fig. 1C predicts a maximal deficit of roughly 4×10^6 sugar molecules. When converted to ATP, this amount is comparable to the internal ATP pool, assuming a conservative estimate of 1–2 ATP per sugar molecule, an intracellular ATP level of 10 mM and an *E. coli* cell volume of 0.5–1 μm^3. While cells have other reserves as well, for example, glycogen and unneeded proteins that can be degraded, the comparison to the ATP pool already indicates that the maximal deficit is very significant for a cell that is deprived of nutrients. In particular, our estimate suggests that a few unprofitable gene inductions triggered by successive environmental changes at unfortunate time points could exhaust all of the remaining resources needed for maintenance of cell viability.

Heterogeneous timing as a bet-hedging strategy

In environments that change in a predictable manner, anticipatory regulation is a beneficial strategy [39,40]. However, in unpredictably fluctuating environments, a cell cannot prevent unprofitable gene induction. Even if, after the environmental change, the cell delays gene induction, it is always possible that the environment changes again shortly afterwards, to a state where the newly induced genes are of no benefit. However, a clonal population of cells can prevent that unprofitable gene induction occurs for all cells, by making sure that different cells choose different delays. The simplest way to achieve this is by having individual cells choose their delay time randomly, from a probability distribution with a suitable width. Such random delays require no communication between cells, only a regulation scheme that exploits gene expression noise. We will discuss a specific mechanism at the end of this paper. First, we examine whether this bet-hedging strategy indeed produces a long-term advantage for a population of cells.

A priori, it is not clear whether heterogeneous timing of gene induction indeed produces a net advantage for cells. A negative consequence of heterogeneous timing is that a fraction of cells is always maladapted for some time after the environmental change. Can this disadvantage be outweighed by the riskreduction mediated by heterogeneous timing? We address this central question by studying heterogeneous timing within an explicit model for the growth and survival of a population of cells in a fluctuating environment. We will see that a trade-off arises between short-term growth, favoring rapid and homogeneous responses, and long-term survival, favoring a heterogeneous response. Toward this end, we first employ a coarse-grained mathematical model that focuses on the essence of this trade-off.

We consider a scenario in which cells experience a series of nutrient pulses interrupted by periods of starvation (Fig. 2A). For simplicity, we assume that the type of nutrient is always different from the one in the previous pulse and can only be accessed through induction of a specialized utilization system. Cells then have to respond to each nutrient pulse to benefit from it, and do not profit from previous inductions in the current pulse [41,42]. We classify nutrient pulses into two types, short (S) and long (L) pulses, which occur with probability p and $1 - p$, respectively (Fig. 2B). S-pulses are too short to yield a net benefit for cells, whereas L-pulses permit cell growth. We also classify the phenotypic response of cells to a pulse into two types of behavior, quick response and delayed response. In each pulse, cells randomly choose their phenotype anew, with q denoting the probability for a cell to respond quickly, such that $1\text{-}q$ is the probability to respond with a significant delay (Fig. 2B).

The effect of a nutrient pulse on a cell depends on both, the type of pulse and the type of cellular response. In Fig. 2C, this dependence is summarized in a "payoff matrix," similar to game theoretical models. However, our model additionally accounts for the internal state of a cell, represented for simplicity by a single variable, the internal "energy level" E, which has a maximal value $E_{\max}$ for an unstressed cell. This energy level changes according to the resource balance of the cell (Fig. 1C). We assume that the duration of an S-pulse falls within the amortization period of the quickly responding cells, whereas it falls within the delay period of the slowly responding cells. The quickly responding cells then suffer an energy deficit, denoted $\varepsilon < 0$, from an S-pulse. By contrast, slowly responding cells effectively never respond to an S-pulse, such that their internal energy level does

not change ($\Delta E = 0$). L-pulses are sufficiently long to replenish the internal energy levels of quick and slow responders alike, and also support growth. Due to the different induction times, quick responders grow by a factor $\gamma > \delta$ that is larger than the growth factor δ of slow responders (Fig. 2C). We assume that cells

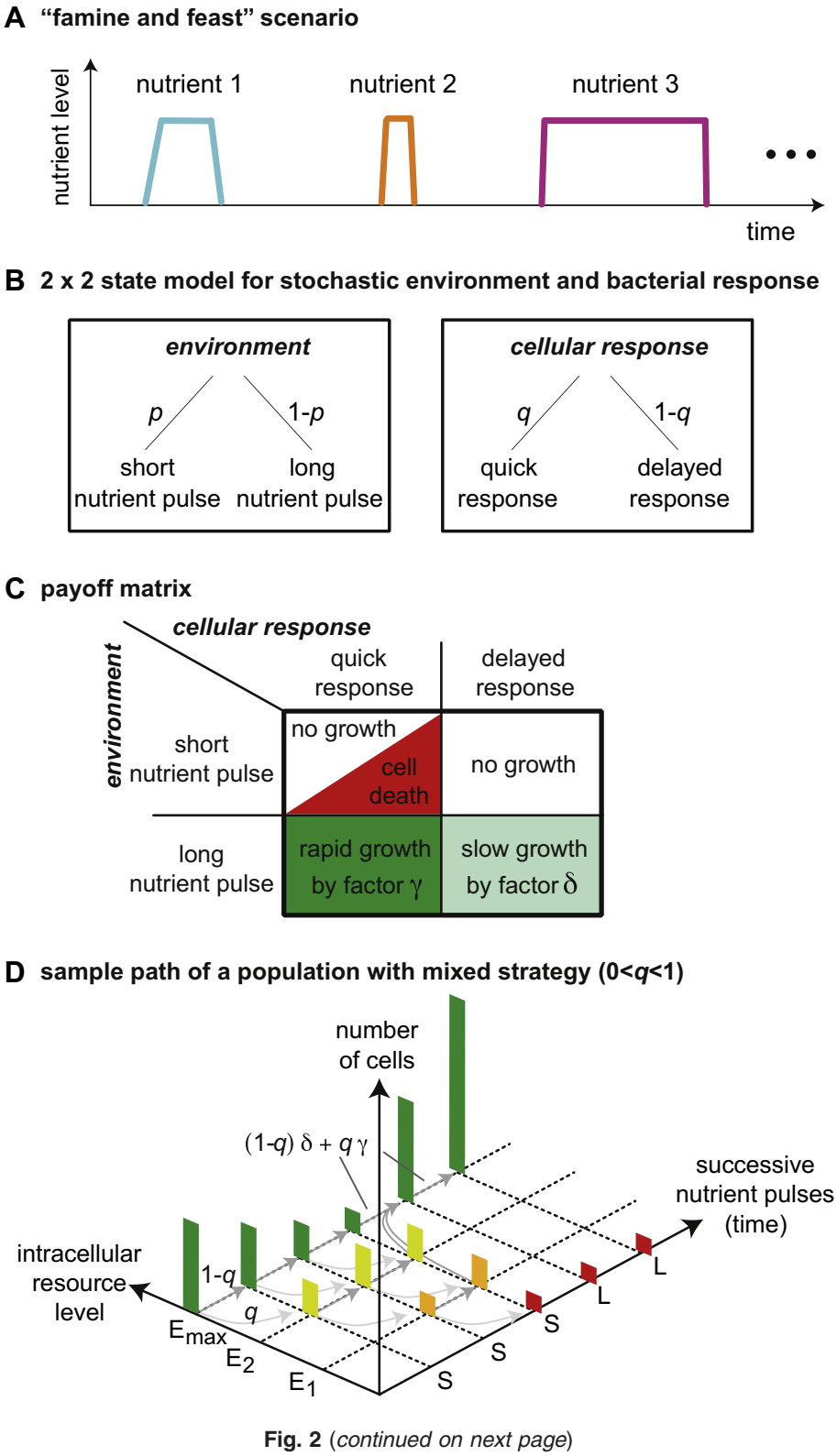

Fig. 2 (*continued on next page*)

keep their internal energy level between nutrient pulses, but when the internal energy of a cell is completely depleted, it is no longer viable. The ratio of the maximal internal energy level E_{max} to the deficit ε controls the number of possible internal energy levels, M, within our model: A cell can be in the M different viable levels E_{max}, $E_{max} - \varepsilon$, $E_{max} - 2\varepsilon$, …, $E_{max} - (M-1)\varepsilon > 0$. When it is in the lowest level, another unprofitable gene induction will kill the cell, $E_{max} - M\varepsilon \leq 0$ The number of energy levels M will effectively be a function of the external nutrient concentration, which affects the magnitude of ε (see Fig. 2C).

Figure 2D illustrates the dynamics of a cell population within this model, by displaying how the cell counts in each energy level evolve over a series of five pulses. Starting from a homogeneous population in the state of maximal energy, heterogeneous timing in the cellular responses generates phenotypic heterogeneity. In the example of Fig. 2D, cells experience three consecutive S-pulses, followed by two L-pulses. We have assumed two intermediate energy states ($M = 2$), denoted E_2 and E_1, in addition to the maximal energy state E_{max}. During the first S-pulse, an average fraction q of cells displays a quick response, consequently suffers an energy deficit, and ends up in state E_2 after the pulse, while the fraction of cells that displays a delayed response remains in the initial state. After the third S-pulse, the fraction of cells that displayed a quick response in each case has entirely depleted its internal energy and is no longer viable. All other cells replenish their internal energy during the following L-pulse and start growing.

It is clear from the example in Fig. 2D that the dynamics of the cell population sensitively depends on the parameter q, which characterizes the regulation strategy of cells. Within the range $0 < q < 1$, cells exhibit a mixed strategy of heterogeneous timing, while the cases of $q = 0$ and $q = 1$ correspond to pure strategies of delayed response and quick response, respectively. The performance of a strategy can be evaluated by calculating the average long-term population growth rate λ, as described in Box 1. This rate quantifies the asymptotic growth of the total number N_T of viable cells with the number T of nutrient pulses (see Eq. (6) in Box 1).

For an environment with a given statistics of nutrient pulses, that is, a fixed probability p for short pulses, the average long-term population growth rate is a function of the cellular response strategy. The analytical calculation of this function $\lambda(q)$ is shown in Box 1 for the case of $M = 2$ intermediate internal energy levels. Here, the main complication in evaluating $\lambda(q)$ stems from the memory that cells have of their recent nutrient history, reflected by their internal energy level. Therefore, the effect of a given nutrient pulse on the population depends on the stochastic sequence of previous pulse durations. The resulting $\lambda(q)$ in Eq. (10), is therefore an average over all possible such sequences.

As Fig. 3A shows, the average long-term growth rate $\lambda(q)$ is a concave function and displays a maximum at intermediate values of q for a given environmental statistics p. This maximum reflects a trade-off between short-term growth and long-term survival. If all cells play the delayed response strategy ($q = 0$), the population grows at a basal rate $\lambda(0) = (1-p)\log_2\delta$. For small q, the growth advantage of quickly responding cells always outweighs a small risk of cell death, such that $\lambda(q)$ increases with q. At higher q, however, the loss due to cell death eventually becomes dominant, such that the population growth rate decreases and even becomes negative (which would result in the extinction of the whole population in the long run). This behavior is qualitatively the same, regardless of the probability p of short pulses. Clearly, the higher p, the more dangerous is the environment for the population, thus driving the optimal strategy toward a more conservative response of low q (red line). Conversely, the more likely long sugar pulses become (low p), the more beneficial it is to have a large fraction of quickly responding cells in the population (green line).

Figure 3B shows how the optimal response strategy, that is, the probability q_{opt} that maximizes the long-term population growth rate, depends on the probability p of a short pulse and the ratio γ/a of growth factors (again for two internal energy states).

Fig. 2. Coarse-grained model for growth and survival in an unpredictable environment. (A) In a natural growth scenario, periods of famine (no nutrient) are interrupted by periods of feast (nutrient available). (B) Simple binary model capturing the essential features of the famine and feast scenario. (C) The payoff matrix relates the growth factors μ (cf. Eq. (7)) to all combinations of nutrient pulse durations and cell responses: Upon long nutrient pulses, cells reproduce either by a factor $\mu = \gamma$ (for cells that quickly induce gene expression) or by a factor $\mu = \delta$ (for cells that induce gene expression at a delay). The energy deficit of a cell responding quickly in a short sugar pulse is only a fraction of the maximal internal energy, such that cells do not suffer immediately from short sugar pulses. However, cells in the lowest (critical) energy level die if they respond quickly in a short sugar pulse. (D) In a mixed strategy, only the quickly responding subpopulation (fraction q) loses energy upon short sugar pulses (S), whereas the energy level of the delayed subpopulation (fraction $1 - q$) remains unchanged. Cells reaching the lowest energy level cannot resume growth (=dead cells), whereas cells with intermediate energy levels do grow upon long sugar pulses and reach the highest energy level E_{max}. Long sugar pulses (L) on the other hand cause population growth by a factor $(1 - q)\delta + q\gamma$.

Box 1
Long-term population growth rate

The long-term population growth rate λ is defined through

$$\lambda = \lim_{T\to\infty} \frac{1}{T} \log_2 \frac{N_T}{N_0}, \qquad (6)$$

where time T is a discrete measure for the number of nutrient pulses and the total population size N_T after T pulses is described by a Markov chain

$$N_T = \mu_T N_{T-1} = N_0 \prod_{i=1}^{T} \mu_i, \qquad (7)$$

with N_0 the initial population size. Here μ_i is the stochastic factor by which the population grows in pulse i. The μ_i depend both on the realization of the environment (short or long pulse, abbreviated as S- or L-pulse, respectively) and on the fraction q of cells that responds with the quick strategy (see below). By combining Eqs. (6) and (7), the long-term growth rate can be expressed as an average over all logarithmic growth factors, that is,

$$\lambda = \lim_{T\to\infty} \frac{1}{T} \sum_{i=1}^{T} \log_2 \mu_i \equiv \overline{\log_2 \mu}. \qquad (8)$$

However, since cells contain a certain memory about their history in the form of their internal energy level, the growth factors depend not only on the duration of the current pulse but also on the stochastic sequence of all previous pulse durations: The more short pulses arrive in a row ("S-chain"), the more dangerous the environment gets for the population. For instance, the sequence SLSLSL is harmless with respect to extinction of a population, since long sugar pulses reset all cells to the highest energy level in every second sugar pulse, whereas the sequence LLLSSS causes the death of cells that respond quickly during the last three pulses (for M = 2).

Consequently, the average of the logarithmic growth factors in Eq. (8) has to be taken over all possible sequences of pulses. The analysis simplifies, however, by noting that a long pulse always resets the whole population to the highest energy level and thereby "erases" the memory of all cells. Hence, during long pulses, which occur with probability 1 − p, the population always grows by a factor $\mu_L(q) = (1 - q)\delta + q\gamma$. In contrast, the survival of a short sugar pulse depends on the history of previous pulse durations, and we have to average over all sequences of S-chains. The probability to find the sequence LS^nL, that is, the probability to have exactly n short pulses in a row, is given by $(1 - p)\, p^n (1 - p)$. The associated growth (or survival) factor is determined by the fraction of cells, which responded quickly at most twice within the S-chain of length n (for M = 2); that is,

$$\mu_{S^n}(q) = \sum_{k=0}^{2} \binom{n}{k} q^k (1-q)^{n-k}. \qquad (9)$$

With this, the long-term population growth rate in Eq. (8) takes the form.

$$\lambda(q) = (1-p)\log_2 \mu_L(q) + (1-p)^2 \sum_{n=3}^{\infty} p^n \log_2 \mu_{S^n}(q). \qquad (10)$$

Thereby, Fig. 3B characterizes the behavior of the coarse-grained model of Fig. 2 over a broad parameter range. Note that q_{opt} never reaches the boundary values zero or one; that is, a heterogeneous strategy always outperforms the pure strategies of delayed response and quick response. For more internal energy states, it will also always be favorable to have a certain fraction of quickly responding cells, since additional internal energy states provide a buffer against unfortunate sequences of short sugar pulses. For completeness, we note that the qualitative behavior of the coarse-grained model changes when we consider the extreme case of just a single intermediate level ($M = 1$). In that limit, a regime emerges where a homogeneous delayed response is optimal. This case is of theoretical interest, since the model then becomes similar to Kelly's problem of optimal gambling [43,44]. We will present a full theoretical analysis of this and other extensions of the current work elsewhere.

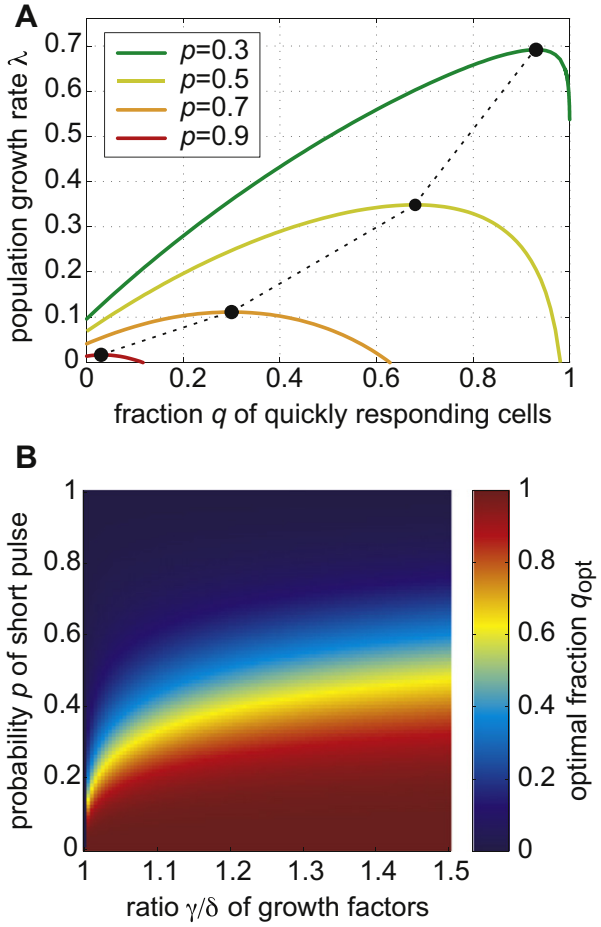

Fig. 3. Optimal response strategies in the coarse-grained model for growth and survival. (A) The population growth rate λ is maximal for mixed strategies, in which the population splits into a quickly and a slowly responding subpopulation ($0 < q < 1$). The higher the probability p of short sugar pulses in the environment, the lower is the optimal fraction of quickly responding cells (black dots). The model parameters are $M = 2$ internal energy states and $\gamma/\delta = 2$, with $\gamma = 2.2$ and $\delta = 1.1$. (B) Dependence of the optimal fraction of quickly responding cells on model parameters for $M = 2$ internal energy states.

Taken together, the analysis of the coarse-grained model of Fig. 2 has shown that the advantage of heterogeneous timing (reduction of the risk of cell death) can outweigh its disadvantage (a fraction of cells is transiently maladapted after environmental changes). However, another key question cannot be addressed within the coarse-grained model, due to its simplified nature with only two pulse lengths and cellular response options: How much variability in the induction times should cells display; that is, what is the optimal width of the delay time distribution? To address this question, we now turn to a model that allows for a continuous range of delay times.

How much variability in induction times is optimal?

In the examples where heterogeneous timing of gene induction has been observed experimentally, the time delays τ of cells spanned a continuum range, as in the distribution shown in Fig. 1B. The most important characteristic of the delay time distribution $P(\tau)$ is its width, which measures the variability in gene induction times. Intuitively, a very large width should be disadvantageous, since a large fraction of cells would then spend a long time in a maladapted state after an environmental transition. On the other hand, a very small width should also be disadvantageous, given that heterogeneous timing mitigates the risk of energy deficits from gene induction, as we have seen above, and heterogeneous timing cannot be effective if the width is too small. Hence, one would expect an intermediate width to be optimal.

In order to test if there is indeed an optimal width and what sets its timescale, we turn to a more fine-grained version of the model considered above. In particular, we allow for a continuous delay time distribution $P(\tau)$, with which we can examine the effects of varying the mean and the variance of the delay time. For this purpose, it is sufficient to use a uniform distribution between a minimal and maximal delay time, $\tau_{min} < \tau < \tau_{max}$, as shown in Fig. 4A. Fluctuations in natural environments will also display a continuum of time scales, so we choose a similar uniform distribution for nutrient pulse durations L, with a maximum L_{max} but no minimum duration (see Fig. 4A and Methods). As a consequence, the energy deficit in a short pulse will also take on continuous values, leading to a whole spectrum of internal energy states within the population. Similarly, there is now a continuum range of growth factors, depending on the time delay of a cell and the duration of the nutrient pulse. As detailed in Methods, we study this continuous model with the help of numerical simulations.

To put our model into the relevant regime, we set the parameters such that an average nutrient pulse permits growth for quickly responding cells. Specifically, we take the nutrient concentration of pulses to be $S = 0.2$ mM, for which the amortization time is about 55 min with the parameters of Fig. 1C, and set the maximal duration L_{max} of pulses to 3 h. We then scan a range of values for τ_{min} and τ_{max} to vary the mean delay time $\langle\tau\rangle$ between 0 and 100 min, and its standard deviation σ between 0 and $\sigma_{max} = \langle\tau\rangle/\sqrt{3}$, the maximal standard deviation obtainable given a uniform distribution with mean $\langle\tau\rangle$.

Figure 4B plots the resulting long-term population growth rates λ as a function of the mean delay time $\langle\tau\rangle$ and the normalized standard deviation σ/σ_{max}. Here, λ is obtained from long-time simulations of the model as described in Methods. Figure 4B can be regarded as a fitness landscape for different regulation strategies, all within the class of

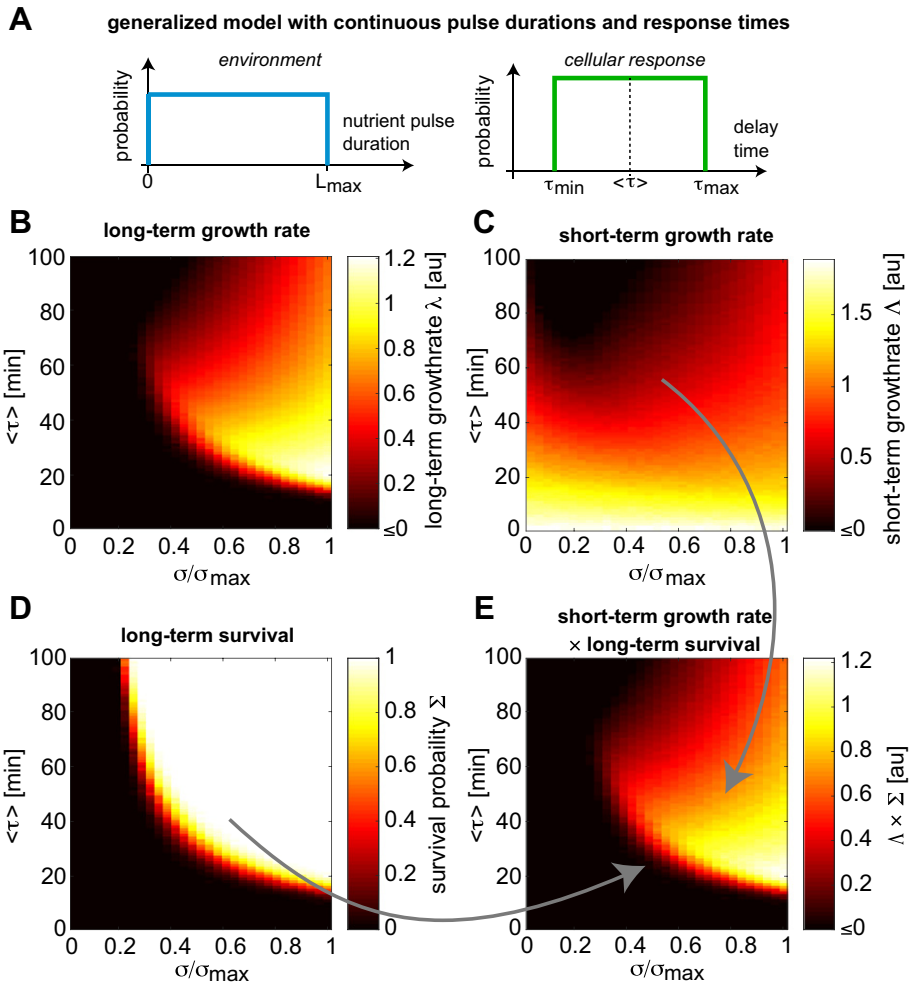

Fig. 4. Continuous model for heterogeneous timing. (A) Growth model with a continuous distribution of nutrient pulse durations and cellular response times. (B) The long-term growth rate λ was simulated over 50,000 nutrient pulses and is shown as a function of the average $\langle\tau\rangle$ and the standard deviation σ of the distribution of cellular response times. (C) The short-term growth rate Λ measures average population growth simulated over 50 nutrient pulses, whereas the long-term survival probability Σ in panel D measures the fraction of populations surviving 50,000 nutrient pulses. While the short-term growth rate is maximal for the most rapid and homogeneous response strategy ($\langle\tau\rangle = 0$ and $\sigma = 0$), long-term survival is only possible if the population responds with a minimal width and average response time. The product of short-term growth rate and long-term survival probability (E) is almost indistinguishable from the long-term growth rate in panel B, suggesting that a trade-off between short-term growth and long-term survival determines the overall fitness of the population. All data in panels B–D were obtained from the average of $N_{avg} = 1000$ independent simulations, see Methods for all details. The maximal environmental pulse duration was chosen to be $L_{max} = 3$ h at a nutrient concentration of $S = 0.2$ mM; all other simulation parameters are as chosen in Fig. 1C.

heterogeneous timing, but differing in their timing statistics. Black areas in the graph correspond to growth rates of zero or less and thus represent non-viable strategies. We observe a pronounced peak in the landscape at average delay times $\langle\tau\rangle$ of around 20 min and the maximal possible variability. Note that the maximal variability corresponds to a delay time distribution that ranges from zero to $2\langle\tau\rangle$, that is, the optimal distribution has a total width of around 40 min, smaller but comparable to the amortization time of 55 min.

Before studying the relation between the optimal width and the amortization time, we focus on the trade-off that underlies the shape of the fitness landscape. Figure 4C shows the same type of plot as Fig. 4B, but with the average growth rate determined over a short time of only a few pulses (see Methods for details). This short-term growth rate, denoted Λ, is maximal when the delay time is zero, that is, when cells respond immediately to a pulse, without variability. Why the long-term growth rate λ displays a different behavior is revealed by inspecting the

survival probability of populations. We quantify the survival probability as the fraction of populations that has not reached population size zero by the end of the simulation. Figure 4D plots the long-term survival probability Σ for the same parameters as the long-term growth rate in Fig. 4B. This survival probability exhibits a sharp ridge, where Σ drops from one to zero when the variability of delay times is too small. In contrast, the short-time survival probability corresponding to Fig. 4C is always almost 100%, since a fatal series of nutrient pulses is very unlikely to occur in the short term.

That the long-term growth rate λ results from a trade-off between short-term growth and long-term survival is seen in Fig. 4E. This panel shows the product of the short-term growth rate Λ and the long-term survival probability Σ, yielding a plot that resembles the long-term growth rate λ in Fig. 4B. Intuitively, this approximate factorization corresponds to a separation between the effects of typical events and the effects of atypical, catastrophic events. The typical growth behavior is sampled already over a short observation time and then does not change. In contrast, a short observation time does not suffice to reveal the effects of rare events, and the probability to encounter catastrophic events increases with observation time.

Figure 5 shows that even with the finite observation time of our simulations, there is a clear connection between the amortization time and the optimal width of the delay time distribution. We varied the external nutrient concentration S in our model to change the amortization time τ_a according to Eq. (3). For each value, we then optimized the long-term growth rate λ as above. As in the case of Fig. 4B, we found optimal distributions with maximal width at a certain average delay $\langle\tau\rangle$. The circles in Fig. 5 show a scatter plot of the amortization times τ_a against the corresponding full widths $2\langle\tau\rangle$ of the optimal delay time distribution. As seen by comparison to the black line (slope one and offset of ≈ 19 min), this scatter plot is compatible with a linear relationship over a broad range. At very low nutrient concentrations (corresponding to large amortization times), the optimal distributions deviate from the linear relationship. This behavior reflects the fact that at very low nutrient concentrations, gene induction no longer results in a net benefit; that is, it is best for cells to not respond to the pulses at all.

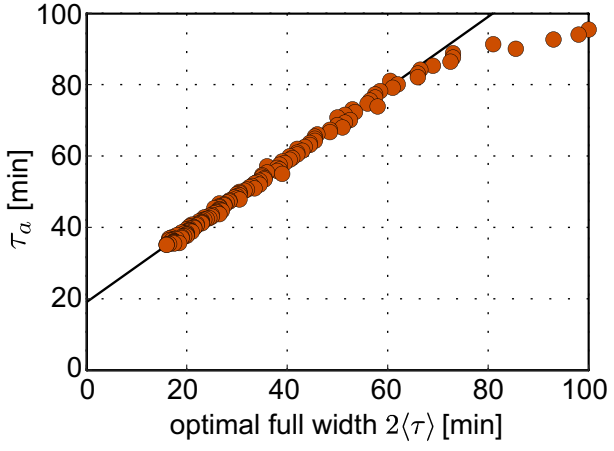

Fig. 5. Correlation between the optimal heterogeneity in timing of gene induction and the theoretically expected amortization time τ_a. The data on the *x*-axis represent the optimal full width ($2\langle\tau\rangle$) of the delay time distribution simulated with the model of Fig. 4 at different nutrient concentrations, while the data on the *y*-axis represent the theoretical expectation of the amortization time (Eq. (3)) at the same nutrient concentration and under identical parameters (parameters are chosen as in Fig. 4). The black line shows a linear correlation with slope 1 and a *y*-axis intercept of 19 min.

Returning to the long-term survival probability of Fig. 4D, it is now clear that in the limit of infinite observation times, the survival of a population is guaranteed only with a heterogeneous timing regulation strategy, in which the total width of the delay time distribution is at least as broad as the amortization period. If this is the case, some cells do not commit themselves to gene induction before others have fully recovered their investment.

Discussion

Up to this point, we established a functional interpretation of the phenomenon of heterogeneous timing, as a microbial strategy to mitigate the risk of energy deficits incurred by responsive gene induction in fluctuating environments. The central concept of this interpretation is the amortization time for the production of enzymes, which emerges from the time-dependent cost–benefit analysis depicted in Fig. 1C. To illustrate the concept, we used the example of a carbon utilization system, for which the benefit can be quantified in terms of the carbon carrying molecules provided by the enzymes of the system. However, our main conclusion is more broadly applicable: Heterogeneous timing can be advantageous as a bet-hedging strategy whenever resources are scarce, such that the costs of gene induction are significant, and the environment fluctuates rapidly and unpredictably. For instance, when a starving population of cells is suddenly exposed to an additional stress, for example, due to a change in osmotic conditions or pH, the induction of the corresponding stress response system will reduce the death rate but is costly. This situation will lead to an amortization time similar to Eq. (3), that is, expressed as a ratio of the cost of the stress response system to the rate of recovering this cost, but with different specific parameters.

We found that heterogeneous timing eliminates the risk of energy deficits, if the width of the delay

time distribution reaches the amortization time. With an even wider distribution, cells would on average spend more time in a maladapted state than necessary for bet-hedging, reducing the long-term growth rate of a population. Hence, delay time distributions with a width comparable to the amortization time are optimal. The key question is then a question of numbers: What are the actual amortization times for inducible systems under different environmental conditions? Our estimates for the case of carbon utilization systems indicated amortization times of several tens of minutes at low nutrient concentrations, comparable to the observed spread in response times of such systems. In the future, it will be important to find ways to probe the amortization dynamics of enzymes experimentally.

Which molecular mechanisms can generate heterogeneous timing and, at the same time, match the width of the delay time distribution to the amortization time of the induced enzymes? While the functional question of the present paper is independent of the molecular mechanisms, we nevertheless want to discuss at least one architecture of a bacterial signaling circuit that can perform this task. First of all, a mechanism for sensing the environmental change that triggers gene induction is required. If the environmental change is reflected in an altered external concentration of a molecule, cells can sense this externally with a receptor (Fig. 6A), or import the molecule with a specific transporter and sense it internally (Fig. 6B). A third option, flux-sensing [45], will not be considered here. Carbon utilization systems, such as the arabinose utilization system depicted in Fig. 6C, typically use internal sensing. It was previously shown that this architecture naturally leads to heterogeneous timing of the cellular response [24].

Conceptually, the underlying mechanism is the "integrate-and-fire" mechanism illustrated in Fig. 6D. The cellular response, that is, gene induction, is triggered when the intracellular concentration of the signal molecule reaches a threshold level. A delay results from the time needed to reach the threshold. The duration of this delay depends on the rate at which the signal molecule is imported, which is proportional to the number of transporters. However, since these transporters are only basally expressed in the uninduced state, there is a considerable cell-to-cell variation in their number, and hence a similar cell-to-cell variation in the delay times. A mathematical model of this mechanism describes the experimentally observed delay time distributions quantitatively [24,25]. A theoretical analysis of timing heterogeneity in a more general class of models is carried out in Ref. [46].

Signaling circuits based on external sensing could produce a variable delay in the cellular response as well, given that many sensors and response regulators also have low copy numbers and considerable noise [47,48]. However, a noteworthy feature of the internal sensing circuit is that it makes the timescale of the delay time distribution inversely proportional to v_S, the rate at which the induced system provides nutrients [24]. As a consequence, the delay time distribution displays the same scaling with nutrient concentration as the amortization time, Eq. (3). In other words, if the width of the delay time distribution is matched to the amortization time at one nutrient concentration, it will automatically remain matched at all nutrient concentrations. In that sense, internal sensing can be considered as an efficient strategy to auto-adapt the variability in induction times.

From a theoretical perspective, it will be interesting to generalize the existing theoretical framework of optimal adaptive strategies for populations in fluctuating environments (see, e.g., Ref. [49] and references therein) to encompass also the case considered here. Toward this end, it will be necessary, for instance, to allow for risks that depend non-trivially on the duration of environmental fluctuations and for the possibility of heterogeneous timing as an adaptive strategy. Finally, another aspect in the analysis of regulation strategies is their evolutionary stability. It is not clear whether heterogeneous timing can be evolutionarily stable. On short timescales, a strategy with high risk displays a larger growth rate in fluctuating environments than strategies with lower risk. If such a high-risk strategy fixates in the population before a sequence of unfortunate pulses diminishes its frequency, the same rare sequence could cause full extinction of the population [50]. However, the involved timescales, the population structure in the ecosystem, and various other factors influence the evolutionary stability of strategies, and we feel that this will be an interesting aspect for future research.

Methods

Continuous growth model

Our continuous growth model assumes a stochastically fluctuating environment with independent pulses of equal nutrient concentration, where the duration L of each pulse is drawn from the homogeneous distribution

$$w(L) = \begin{cases} 1/L_{max} & 0 \le \mathrm{L} \le L_{\max} \\ 0 & \text{otherwise} \end{cases}$$

Each cell responds to a pulse with a stochastic delay time τ that is also drawn from a homogeneous distribution,

$$P(\tau) = \begin{cases} 1/(\tau_{\max}-\tau_{\min}) & \tau_{\min} \le \tau \le \tau_{\max} \\ 0 & \text{otherwise} \end{cases}$$

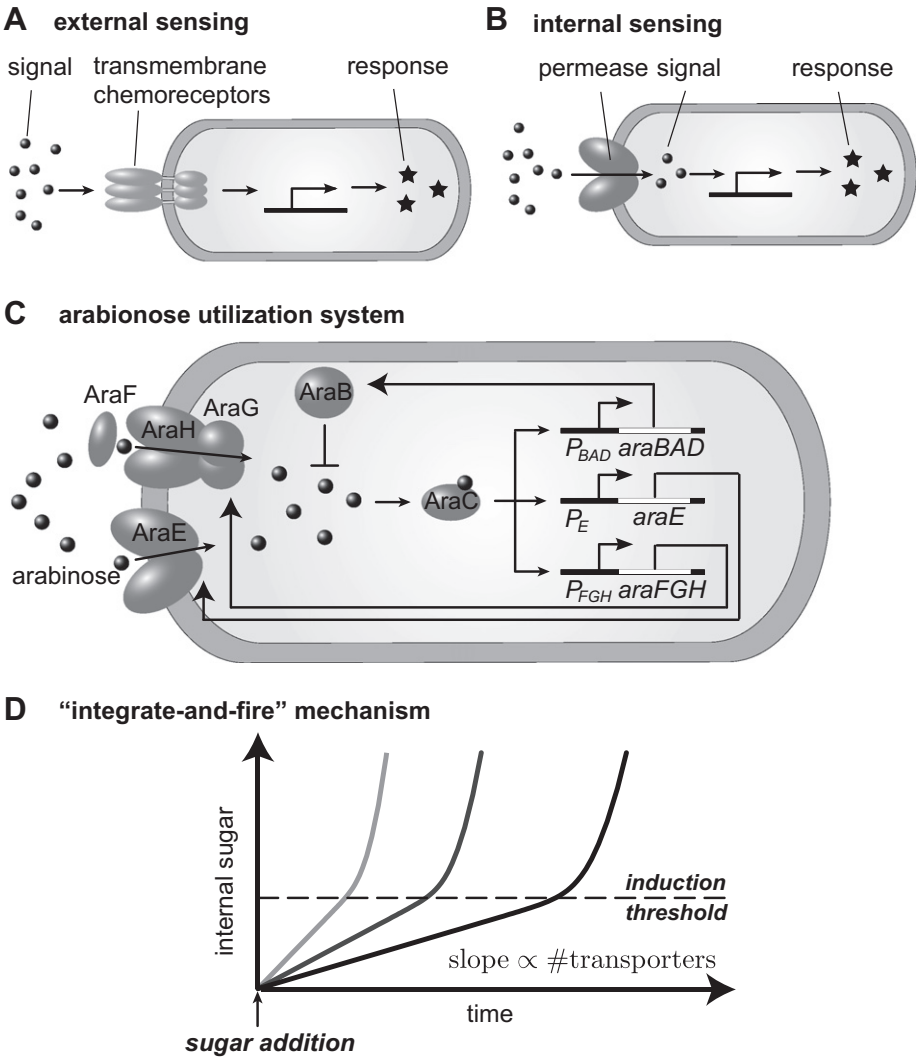

Fig. 6. A mechanism for heterogeneous timing. (A, B) Responsive gene induction requires a sensing mechanism. External (A) and internal (B) sensing are the principal options. (C) Schematic diagram of the arabinose utilization system in *E. coli* which employs internal sensing: External arabinose is imported via specific transporters (AraE, AraFGH) to the cytoplasm, where it activates transcription of the transporters and the required enzymes (AraBAD) via the transcription factor AraC. (D) The architecture of the signaling circuit effectively implements an "integrate-and-fire" mechanism for heterogeneous timing of gene induction: Cells accumulate internal nutrient at a rate proportional to the number of basally expressed transporter proteins ("integrate") until the binding threshold K_S for activation of the genes in the carbon utilization system is reached ("fire"). Cell-to-cell variability in the initial number of transporters leads to a broad distribution of induction times.

The energetic state of cells is characterized by a continuous internal variable C, which ranges from zero to $C_{\max}$. Upon induction of the nutrient utilization system, the internal state of each cell follows the parabolic dynamics of Eq. (2) until the pulse ends or the maximal level $C_{\max}$ is reached. From then on, cells grow at a constant doubling rate λ_0 for as long as nutrient is still present. Cells that due to unprofitable gene induction reach the state $C = 0$ are considered non-viable.

Assuming large population sizes, we treat the total size of the population N_t after the t-th pulse as a continuous variable. The state of the cell population after the t-th pulse is specified by the density $n_t(C)$ over the internal states C. The total number of cells then is

$$N_t = \int_0^{C_{\max}} \mathrm{d}C\, n_t(C).$$

For our numerical simulations, we store the distributions $n_t(C)$ and $P(\tau)$ in finite arrays with f components, where f was chosen sufficiently large

($f > 200$) to make discretization effects negligible. The stochastic dynamics of the model was implemented as follows. Given the population state $n_t(C)$ after the t-th pulse, we first divide the population into subpopulations with nutrient level C, delay time τ, and size $n_t(C,\tau) \coloneqq n_t(C) \times p(\tau)$. We then draw a pulse duration L randomly from $w(L)$ and obtain the state $n_{t+1}(C)$ by the following update procedure: For each subpopulation, we calculate the time $t_{\max}$ at which the internal state $C_{\max}$ would be reached; that is,

$$t_{\max} = \tau + \frac{1}{v_S}\left[a + \sqrt{a^2 + 2v_S(C_{\max} - C)/k_p}\right].$$

If $L \geq t_{\max}$, the subpopulation reaches the maximal energetic state $C_{\max}$ and grows by a factor $\mu(C,\tau) = 2^{\lambda_0(L-t_{\max})}$. In contrast, if $L < t_{\max}$, the subpopulation reaches the energetic state $C + \Delta C(L)$ and does not grow. Here, $\Delta C(L)$ is defined through Eq. (2) if cells respond before the nutrient pulse ends ($\tau < L$), and is zero if the delay time is at least as long as the nutrient pulse ($\tau \geq L$). If $C + \Delta C(L) \leq 0$, we set the size of this subpopulation to zero (cells die), while the size remains unchanged otherwise. We obtain $n_{t+1}(C)$ by summing over all subpopulations with different delays τ but the same energetic state C.

To characterize the typical behavior of cell populations, we perform a large number N_{avg} of simulation runs, for a period of T pulses each. This yields the final population sizes $N_{T,i}$ with the index i denoting the simulation run ($i = 1 \ldots N_{\text{avg}}$). Based on these data, we then compute two observables, which quantify the survival probability and the average growth rate of populations. The survival probability Σ_T is defined as the fraction of populations that have not reached a size of zero; that is,

$$\Sigma_T = 1 - \frac{1}{N_{\text{avg}}}\sum_{i=1}^{N_{\text{avg}}} \delta_{0N_{T,i}} \qquad (11)$$

using the Kronecker delta δ_{ij}. The average growth rate Λ_T is defined as the population average of the time-averaged growth rates,

$$\Lambda_T = \frac{1}{N_{\text{avg}}\Sigma_T}\sum_{i=1}^{N_{\text{avg}}}(1-\delta_{0N_{T,i}})\frac{1}{T}\log_2\frac{N_{T,i}}{N_0}. \qquad (12)$$

In the Results section, we analyze the long-term growth rate λ computed by evaluating Λ_T for $T = 50{,}000$. We also analyze the corresponding long-term survival probability $\Sigma \equiv \Sigma_{50,000}$ and the short-term growth rate $\Lambda \equiv \Lambda_{50}$ computed with $T = 50$ nutrient pulses. The short-term growth rate is dominated by the typical environmental fluctuations, since very few populations encounter a succession of several badly-timed pulses within the short time window, whereas the long-term growth rate includes the effect of such rare events. In contrast, the survival probability is dominated by the rare events. Taken together, this rationalizes the approximate factorization observed in Fig. 4E.

Acknowledgments

It is a pleasure to thank Erik Aurell and Massimo Vergassola for stimulating discussions. This work was supported by the German Research Foundation through grants GE 1098/6-2 and FR 3673/1-2, as well as the Excellence Cluster “Nanosystems Initiative Munich”, and by the State of Hesse (Germany) through the LOEWE program.

Received 31 January 2019;
Received in revised form 25 April 2019;
Available online 26 May 2019

Keywords:
gene regulation strategies;
bet-hedging;
cost–benefit analysis

References

[1] A. Novick, M. Weiner, Enzyme induction is an all-or-none phenomenon, Proc. Natl. Acad. Sci. U. S. A. 43 (1957) 553–566.
[2] P.C. Maloney, B. Rotman, Distribution of suboptimally induced β-D-galactosidase in *Escherichia coli*. The enzyme content of individual cells, J. Mol. Biol. 73 (1973) 77–91.
[3] D.A. Siegele, J.C. Hu, Gene expression from plasmids containing the araBAD promoter at subsaturating inducer concentrations represents mixed populations, Proc. Natl. Acad. Sci. U. S. A. 94 (1997) 8168–8172.
[4] S.R. Biggar, G.R. Crabtree, Cell signaling can direct either binary or graded transcriptional responses, EMBO J. 20 (2001) 3167–3176.
[5] R. Losick, C. Desplan, Stochasticity and cell fate, Science 320 (2008) 65–68.
[6] A. Raj, A. van Oudenaarden, Nature, nurture, or chance: stochastic gene expression and its consequences, Cell 135 (2008) 216–226.
[7] H.B. Fraser, A.E. Hirsh, G. Giaever, J. Kumm, M.B. Eisen, Noise minimization in eukaryotic gene expression, PLoS Biol. 2 (2004) e137.
[8] E. Korobkova, T. Emonet, J.M.G. Vilar, T.S. Shimizu, P. Cluzel, From molecular noise to behavioural variability in a single bacterium, Nature 428 (2004) 574–578.
[9] D. Fraser, M. Kæ–rn, A chance at survival: gene expression noise and phenotypic diversification strategies, Mol. Microbiol. 71 (2009) 1333–1340.
[10] Z. Zhang, W. Qian, J. Zhang, Positive selection for elevated gene expression noise in yeast, Mol. Syst. Biol. 5 (2009) 299.
[11] A. Eldar, M.B. Elowitz, Functional roles for noise in genetic circuits, Nature 467 (2010) 167–173.

[12] N.Q. Balaban, J. Merrin, R. Chait, L. Kowalik, S. Leibler, Bacterial persistence as a phenotypic switch, Science 305 (2004) 1622–1625.
[13] M. Acar, J.T. Mettetal, A. van Oudenaarden, Stochastic switching as a survival strategy in fluctuating environments, Nat. Genet. 40 (2008) 471–475.
[14] H.J.E. Beaumont, J. Gallie, C. Kost, G.C. Ferguson, P.B. Rainey, Experimental evolution of bet hedging, Nature 462 (2009) 90–93.
[15] P. Paszek, S. Ryan, L. Ashall, K. Sillitoe, C.V. Harper, D.G. Spiller, D.A. Rand, M.R.H. White, Population robustness arising from cellular heterogeneity, Proc. Natl. Acad. Sci. U. S. A. 107 (2010) 11644–11649.
[16] J.-W. Veening, E.J. Stewart, T.W. Berngruber, F. Taddei, O. P. Kuipers, L.W. Hamoen, Bet-hedging and epigenetic inheritance in bacterial cell development, Proc. Natl. Acad. Sci. U. S. A. 105 (2008) 4393–4398.
[17] D. Lopez, H. Vlamakis, R. Kolter, Generation of multiple cell types in *Bacillus subtilis*, FEMS Microbiol. Rev. 33 (2009) 152–163.
[18] C. Anetzberger, T. Pirch, K. Jung, Heterogeneity in quorum sensing-regulated bioluminescence of *Vibrio harveyi*, Mol. Microbiol. 73 (2009) 267–277.
[19] M. Thattai, A. van Oudenaarden, Stochastic gene expression in fluctuating environments, Genetics 167 (2004) 523–530.
[20] E. Kussell, S. Leibler, Phenotypic diversity, population growth, and information in fluctuating environments, Science 309 (2005) 2075–2078.
[21] E.M. Ozbudak, M. Thattai, H.N. Lim, B.I. Shraiman, A. van Oudenaarden, Multistability in the lactose utilization network of *Escherichia coli*, Nature 427 (2004) 737–740.
[22] M. Acar, A. Becskei, A. van Oudenaarden, Enhancement of cellular memory by reducing stochastic transitions, Nature 435 (2005) 228–232.
[23] B.B. Kaufmann, Q. Yang, J.T. Mettetal, A. van Oudenaarden, Heritable stochastic switching revealed by single-cell genealogy, PLoS Biol. 5 (2007) e239.
[24] J.A. Megerle, G. Fritz, U. Gerland, K. Jung, J.O. Rädler, Timing and dynamics of single cell gene expression in the arabinose utilization system, Biophys. J. 95 (2008) 2103–2115.
[25] G. Fritz, J.A. Megerle, S.A. Westermayer, D. Brick, R. Heermann, K. Jung, J.O. Rädler, U. Gerland, Single cell kinetics of phenotypic switching in the arabinose utilization system of *E. coli*, PLoS One 9 (2014), e89532.
[26] M. Leisner, J.-T. Kuhr, J.O. Rädler, E. Frey, B. Maier, Kinetics of genetic switching into the state of bacterial competence, Biophys. J. 96 (2009) 1178–1188.
[27] A. Mutlu, S. Trauth, M. Ziesack, K. Nagler, J.-P. Bergeest, K. Rohr, N. Becker, T. Höfer, I.B. Bischofs, Phenotypic memory in *Bacillus subtilis* links dormancy entry and exit by a spore quantity-quality tradeoff, Nat. Commun. 9 (2018) 69.
[28] A. Jõers, T. Tenson, Growth resumption from stationary phase reveals memory in *Escherichia coli* cultures, Sci. Rep. 6 (2016), 24055.
[29] E. Dekel, S. Mangan, U. Alon, Environmental selection of the feed-forward loop circuit in gene-regulation networks, Phys. Biol. 2 (2005) 81–88.
[30] E. Dekel, U. Alon, Optimality and evolutionary tuning of the expression level of a protein, Nature 436 (2005) 588–592.
[31] T. Kalisky, E. Dekel, U. Alon, Cost-benefit theory and optimal design of gene regulation functions, Phys. Biol. 4 (2007) 229–245.
[32] M. Eames, T. Kortemme, Cost–benefit tradeoffs in engineered lac operons, Science 336 (2012) 911–915.
[33] M. Kafri, E. Metzl-Raz, G. Jona, N. Barkai, The cost of protein production, Cell Rep. 14 (2016) 22–31.
[34] C. Kaleta, S. Schäuble, U. Rinas, S. Schuster, Metabolic costs of amino acid and protein production in *Escherichia coli*, Biotechnol. J. 8 (2013) 1105–1114.
[35] S. Sundararaj, A. Guo, B. Habibi-Nazhad, M. Rouani, P. Stothard, M. Ellison, D.S. Wishart, The CyberCell Database (CCDB): a comprehensive, self-updating, relational database to coordinate and facilitate in silico modeling of *Escherichia coli*, Nucl. Acids Res. 32 (2004) D293–D295.
[36] J.K. Wright, P. Overath, Purification of the lactose:H+ carrier of *Escherichia coli* and characterization of galactoside binding and transport, Eur. J. Biochem. 138 (1984) 497–508.
[37] K. Dornmair, P. Overath, F. Jähnig, Fast measurement of galactoside transport by lactose permease, J. Biol. Chem. 264 (1989) 342–346.
[38] K.R. Daruwalla, A.T. Paxton, P.J. Henderson, Energization of the transport systems for arabinose and comparison with galactose transport in *Escherichia coli*, Biochem. J. 200 (1981) 611–627.
[39] I. Tagkopoulos, Y.C. Liu, S. Tavazoie, Predictive behavior within microbial genetic networks, Science 320 (2008) 1313–1317.
[40] A. Mitchell, G.H. Romano, B. Groisman, A. Yona, E. Dekel, M. Kupiec, O. Dahan, Y. Pilpel, Adaptive prediction of environmental changes by microorganisms, Nature 460 (2009) 220–224.
[41] G. Lambert, E. Kussell, Memory and fitness optimization of bacteria under fluctuating environments, PLoS Genet. 10 (2014), e1004556.
[42] A. Skanata, E. Kussell, Evolutionary phase transitions in random environments, Phys. Rev. Lett. 117 (2016), 038104.
[43] J.L. Kelly, A new interpretation of information rate, Bell. Syst. Tech. J. 35 (1956) 917–926.
[44] E. Aurell, R. Baviera, O. Hammarlid, M. Serva, A. Vulpiani, Growth optimal investment and pricing of derivatives, Physica A 280 (2000) 505–521.
[45] G. Fritz, S. Dintner, N.S. Treichel, J. Radeck, U. Gerland, T. Mascher, S. Gebhard, A new way of sensing: need-based activation of antibiotic resistance by a flux-sensing mechanism, mBio 6 (2015) e00975–15.
[46] A. Dal Co, M. Lagomarsino, M. Caselle, M. Osella, Stochastic timing in gene expression for simple regulatory strategies, Nucl. Acids Res. 45 (2017) 1069–1078.
[47] A. Becskei, B.B. Kaufmann, A. van Oudenaarden, Contributions of low molecule number and chromosomal positioning to stochastic gene expression, Nat. Genet. 37 (2005) 937–944.
[48] S.-W. Teng, Y. Wang, K.C. Tu, T. Long, P. Mehta, N.S. Wingreen, B.L. Bassler, N.P. Ong, Measurement of the copy number of the master quorum-sensing regulator of a bacterial cell, Biophys. J. 98 (2010) 2024–2031.
[49] A. Mayer, T. Mora, O. Rivoire, A.M. Walczak, Transitions in optimal adaptive strategies for populations in fluctuating environments, Phys. Rev. E 96 (2017), 032412.
[50] U. Gerland, T. Hwa, Evolutionary selection between alternative modes of gene regulation, Proc. Natl. Acad. Sci. U. S. A. 106 (2009) 8841–8886.